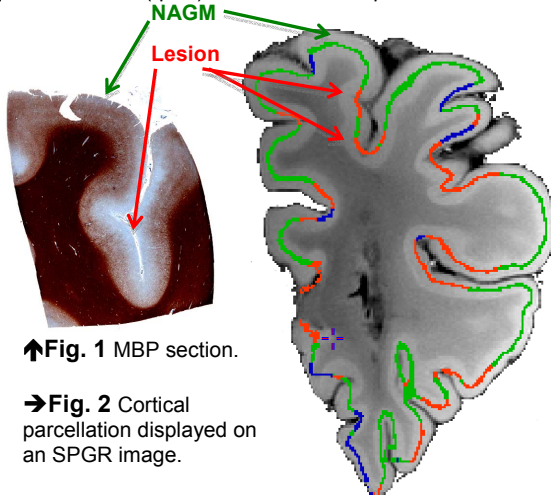


Profile-based cortical parcellation to detection of cortical multiple sclerosis lesions

C. L. Tardif¹, J. B. Richardson², C. Lepage¹, D. L. Collins¹, A. C. Evans¹, and G. B. Pike¹

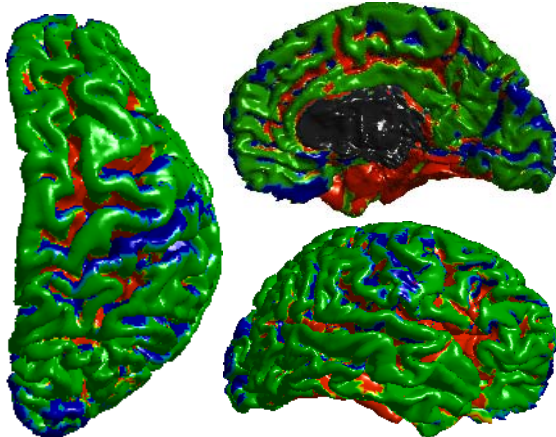
¹McConnell Brain Imaging Centre, Montreal Neurological Institute, Montreal, QC, Canada, ²Department of Neuropathology, Montreal Neurological Institute/Hospital, Montreal, QC, Canada

Introduction Cortical multiple sclerosis (MS) pathology remains notoriously difficult to detect *in vivo* using MRI mainly due to poor contrast between cortical lesions and normal appearing grey matter (NAGM), and partial volume effects with CSF. In addition, the spatial variation in healthy GM, of diffuse pathology and partial remyelination, result in a relatively flat distribution of quantitative MR parameters over the cortex. We propose using an automated profile-based analysis technique for cortical parcellation to detect demyelinated cortical lesions, and show initial results on high-resolution quantitative MR (qMR) data from a fixed *postmortem* MS hemisphere, validated with myelin basic protein (MBP) immunohistochemistry.



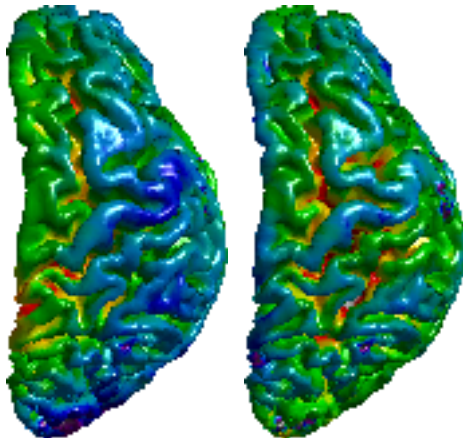
↑Fig. 1 MBP section.

→Fig. 2 Cortical parcellation displayed on an SPGR image.



↑Fig. 3 Cortical parcellation results.

↓Fig. 4 Mid-cortical T1 map and non-uniformity corrected M0 map.



Dev Disord 39, 1568-1581(2009). [6] Walters *et al*, Hum Brain Mapp 28, 1-8 (2007).

Methods The fixed right hemisphere of an MS patient (79 year old female, disease duration 30 years) was provided by the Douglas Hospital Research Centre Brain Bank. Images were acquired on a Siemens Tim Trio 3T MRI scanner with a 32-channel coil. The hemisphere was placed in an MR-compatible cylindrical container filled with 10% buffered formalin. 3D sagittal images were acquired with 0.35mm isotropic resolution, 512x512x240 matrix size and 6/8 partial phase encoding. Quantitative T1, T2 and M0 maps were acquired using DESPOT1 (SPGR: $\alpha/TE/TR/NSA = [4\text{vert}^\circ, 22^\circ]/3.35\text{ms}/7.7\text{ms}/49$) and DESPOT2 (SSFP: $\alpha/TE/TR/NSA = [20^\circ, 70^\circ]/3.84\text{ms}/7.7\text{ms}/49$) [1]. The magnetization transfer ratio (MTR) map was calculated from 2 SPGR acquisitions ($\alpha/TE/TR/NSA = 25^\circ/4.09\text{ms}/25\text{ms}/13$), with and without MT-weighting (500° Gaussian pulse of 10ms, 1200Hz off-resonance, 100Hz bandwidth). We also acquired a 2mm isotropic $\Delta B1$ map from two 2D magnetization-prepared TSE images ($\alpha/TES/TR/\text{Turbo} = [20^\circ, 40^\circ]/15\text{ms}/2\text{s}/7$) to correct the flip angles in the DESPOT techniques. The total acquisition time was of ~55 hours. Tissue blocks were selected for paraffin embedding based on the MR images. Sections were cut at 5 μm and reacted with antibody directed against MBP (DAKO A0623), and processed in a Ventana Benchmark XT with diaminobenzidine as chromogen. Slides were digitized using a Zeiss MIRAX Scan automated slide scanner.

Image processing was performed using the MINC2 tools, CIVET [3], and Matlab, including the SurfStat toolbox [4]. The M0 and T2 maps were non-uniformity corrected for RF reception and banding artifacts respectively. The MTR map was aligned to the right hemisphere of the ICBM-152 non-linear atlas, and discretely classified. The classification was corrected for partial volume effects, and a CSF skeleton was created. The WM surface was extracted first by deforming an ellipsoid polygonal model as it shrinks inwards. The GM surface was computed by expanding the WM surface outwards towards the CSF skeleton. Cortical profiles were created by sampling 20 points between matching vertices on the WM and GM surfaces using linear interpolation. The first and last 10% of samples were removed to avoid contamination from neighboring tissues. The remaining samples were blurred along the cortical ribbon (2mm FWHM). A 10-parameter feature vector was extracted from each of the 40 962 profiles, including the mean amplitude and first four central moments of the profile and its absolute first derivative [5,6]. The feature vectors derived from the 4 qMR maps (T1, M0, T2 and MTR) were concatenated, for a total of 40 features per profile. Each feature was z-scored to equally weigh the k-means classification. The profiles were classified into 4 clusters using a k-means classifier with a squared Euclidean distance metric.

Results An MBP-stained section of the superior frontal gyrus is shown in Fig. 1, where myelin is stained brown. The light subpial band along the sulcus corresponds to a demyelinated cortical MS lesion. The corresponding cortical parcellation results are shown in Fig. 2. The subpial lesion at the base of the sulcus (red label) was automatically segmented from the neighboring NAGM (green label). The cortical parcellation results of the whole hemisphere are shown in Fig. 3. The areas labeled as lesion in red are mainly located deep in the sulci of the frontal, temporal, insular and cingulate cortices. These areas are characterized by an increase in T1 and M0, as seen on the mid-cortical surfaces in Fig. 4. The blue label in Fig. 3 corresponds to cortical areas that are more densely myelinated, in particular in the motor and visual cortices. The black label corresponds to the non-cortical tissue.

Discussion This observer-independent cytoarchitecture analysis method was previously applied to high-resolution MRI to parcellate the visual cortex [6]. The technique is well suited for the detection of subpial MS lesions due to their morphology. The main source of error is inaccuracy in tissue classification (into WM, GM and CSF), and subsequent surface extraction. The techniques could be improved by increasing the number of vertices on the surface, and by applying Laplacian fluid dynamics to extract the profiles. The main limitations of this technique for *in vivo* MRI will be the resolution of the images.

References [1] Deoni, *et al*, Magn Reson Med 53, 237-241 (2005). [2] Sled & Pike, Magn Reson Med 43, 589-593 (2000). [3] Ad-Dab'bagh *et al*, HBM proceedings (2006). [4] Chung *et al*, Info Proc in Med Imag 19, pp. 627-638 (2005). [5] Schleicher *et al*, J Autism